IMA Journal of Applied Mathematics (1994) **52,** 79–92

On the speed of amplitude transition waves in reaction–diffusion systems of λ–ω type

JONATHAN A. SHERRATT

Nonlinear Systems Laboratory, Mathematics Institute, University of Warwick, Coventry CV4 7AL, UK

AND

Centre for Mathematical Biology, Mathematical Institute, 24–29 St Giles', Oxford OX1 3LB, UK

[Received 12 April 1993]

λ–ω systems are a class of simple examples of two coupled reaction–diffusion equations whose kinetics have a stable limit cycle. The author considers the evolution of such systems from simple initial data in which a small homogeneous perturbation is applied to the unique steady state in a localized region of the domain. Using a combination of analytical and numerical methods, it is shown that the system evolves to two sets of transition wave fronts in the solution amplitude, one moving outwards from the perturbation, and the other moving inwards. An expression is derived for the speed of the outward moving wave, and it is shown that this in turn determines the speed of the inward moving wave. Between these transition fronts, the solution has the form of periodic plane waves, whose amplitude is the solution of a simple algebraic equation. In some cases these periodic plane waves are unstable as reaction–diffusion solutions, in which case they degenerate into irregular spatiotemporal oscillations.

1. Introduction

'λ–ω systems' are a class of simple examples of two coupled reaction–diffusion equations whose kinetics have a stable limit cycle:

$$u_t = u_{xx} + \lambda(r)u - \omega(r)v, \qquad v_t = v_{xx} + \omega(r)u + \lambda(r)v. \tag{1.1a,b}$$

Here u and v are functions of space x and time t, with $x \in \mathbb{R}$ and $t > 0$, and $r = (u^2 + v^2)^{\frac{1}{2}}$; the subscripts x and t denote partial derivatives. Numerous previous authors have used λ–ω systems to investigate periodic plane waves (Kopell & Howard, 1973; Ermentrout, 1980) and spiral waves (Greenberg, 1981; Koga, 1982). These solution types are characteristic of reaction–diffusion systems with a limit cycle in the kinetics, but are hard to analyse in general systems of this type, so that λ–ω systems are used as a prototype. In contrast to this detailed study of particular solution types, there has been very little previous work on the way in which the solution of (1.1) evolves from given initial conditions. A notable exception is a paper by Lange & Larson (1980), in which a multiple timescale procedure is used to obtain an asymptotic expansion for the solution when the initial data varies slowly with x, in the specific case $\lambda(r) = 1 - r$ and $\omega(r) \equiv 1$. Here I investigate the way in which the solution of (1.1) evolves following a

small perturbation of the steady state $u = v = 0$. Throughout the paper I will assume that $\lambda(\bullet)$ is strictly decreasing, with a simple zero at $r = r_L > 0$, and that $\omega(0) > 0$. The kinetic ordinary differential equations then have a unique steady state at $u = v = 0$, which is an unstable spiral, and there is a circular limit cycle of radius r_L, which is globally attracting. For the majority of the paper I will further assume that $\omega(\bullet)$ is strictly decreasing, although I will relax this condition slightly in Section 4. I also take the boundary conditions at $x = \pm\infty$ to be $u_x = v_x = 0$. The limit cycle of the kinetics is then a (spatially homogeneous) solution of the partial differential equations, and it is straightforward to show that it is linearly stable (Kopell & Howard, 1973).

I consider the evolution of (1.1) from the initial data

$$u(x, 0) = v(x, 0) = \begin{cases} \varepsilon & \text{if } |x| < L, \\ 0 & \text{otherwise,} \end{cases} \tag{1.2}$$

where $\varepsilon \ll r_L$. The dynamics of the reaction kinetics imply that, when $L = \infty$, the solution will tend towards the homogeneous periodic solution

$$u = r_L \cos[\omega(r_L)(t - t_0)], \qquad v = r_L \sin[\omega(r_L)(t - t_0)],$$

where t_0 is a constant determined by ε, and this is illustrated in Fig. 1(a). However, when L is finite, it is not immediately clear what the behaviour will be. I begin by considering the case of L very small, in a sense that will be made clear.

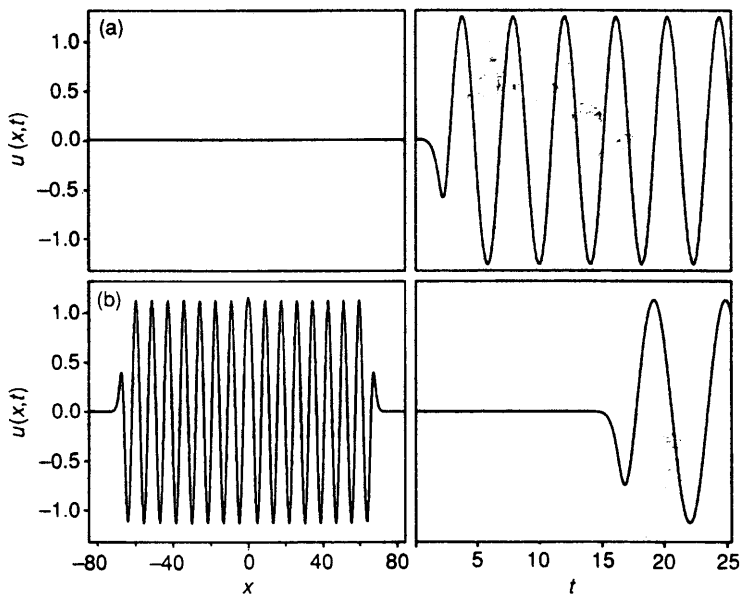

FIG. 1. The solution of (1.1) subject to (1.2), with $\varepsilon = 0.01$ and (a) $L = \infty$ and (b) $L = 2$. In both cases $\lambda(r) = 2 - r^3$ and $\omega(r) = 2 - e^r$, and I plot $u(x, t)$ as a function of x at $t = 25$ and as a function of t at $x = 42$. The solution for v is qualitatively very similar. In (a), the solution evolves to the limit cycle of the kinetics, while in (b) a wave front moves across the domain, with regular spatiotemporal oscillations behind the front. Here and in numerical solutions of the partial differential equations presented in other figures, the system (1.1) was solved numerically using the method of lines and Gear's method, and the solution is essentially independent of ε.

Intuitively, one might expect that there would be a region of homogeneous oscillations expanding from the origin in both the positive and negative x directions. However, numerical solutions suggest that this is not the case. Rather, wave fronts do move out from the site of the perturbation, but the solution behind these fronts consists of regular *spatio*temporal oscillations, of lower amplitude than r_L (Fig. 1(b)).

2. Periodic plane waves

The nature of the spatiotemporal oscillations induced by localized perturbations to $u = v = 0$ is clarified when one plots the solutions for r and θ_x. Here r and θ are polar coordinates in the u–v plane, so that

$$r = (u^2 + v^2)^{\frac{1}{2}}, \qquad \theta = \tan^{-1}(v/u), \qquad \theta_x = (uv_x - vu_x)/(u^2 + v^2).$$

The solution in Fig. 1(b) is replotted in terms of r and θ_x in Fig. 2, revealing transition wave fronts that appear to move with constant shape and speed. Similar numerical results are obtained for a wide range of other (strictly decreasing) functional forms for $\lambda(\cdot)$ and $\omega(\cdot)$. Transition fronts in r and θ_x have previously been studied by Howard & Kopell (1974, 1977) in the case in which r is nonzero on both sides of the front; they showed that there is a 1–1 relationship between

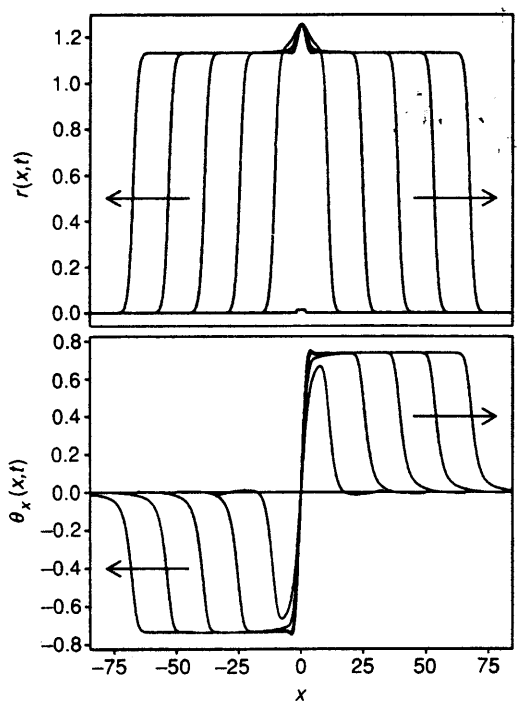

FIG. 2. The solution of (1.1) subject to (1.2) for the functional forms and parameter values as in Fig. 1(b). In this case I plot r and θ_x as functions of x at equally spaced times, including $t = 0$; the time interval is 5. This reveals transition wave fronts moving across the domain with constant shape and speed.

the front velocity and the change in amplitude across the front. I will show that when $r = 0$ ahead of the front, the situation is more complex, but the 1–1 relationship remains.

Taking r and θ as dependent variables, the partial differential equations (1.1) become

$$r_t = r\lambda(r) + r_{xx} - r\theta_x^2, \qquad \theta_t = \omega(r) + \theta_{xx} + 2r_x\theta_x/r. \tag{2.1a,b}$$

I am considering transition front solutions, with θ_x and r tending to constant values behind the front. Denoting these constant values by ψ_s and r_s respectively, (2.1a) implies that $\psi_s^2 = \lambda(r_s)$, which is satisfied by the values observed in numerical solutions of (1.1). Equation (2.1b) then gives $\theta_t = \omega(r_s)$. Therefore, behind the transition fronts, the solution tends towards

$$u = r_s \cos[\omega(r_s)t + \psi_s x + \theta_0], \qquad v = r_s \sin[\omega(r_s)t + \psi_s x + \theta_0], \tag{2.2a,b}$$

where θ_0 is an arbitrary constant. This solution is a periodic plane wave, which moves across the domain with constant shape and speed, oscillating in space and time. Periodic plane wave solutions of λ–ω systems have been extensively studied by previous authors (reviewed by Murray, 1989: Chap. 12). In particular, Kopell & Howard (1973) showed that a periodic plane wave solution of the form (2.2) exists for all $r_s \in (0, r_L)$, and is linearly stable on an infinite spatial domain if and only if

$$4\lambda(r_s)\left[1 + \left(\frac{\omega'(r_s)}{\lambda'(r_s)}\right)^2\right] + r_s\lambda'(r_s) \leq 0. \tag{2.3}$$

Thus waves of sufficiently low amplitude are unstable, while those of sufficiently high amplitude are stable. The development of periodic plane waves following localized perturbations to $u = v = 0$ is illustrated in Fig. 3.

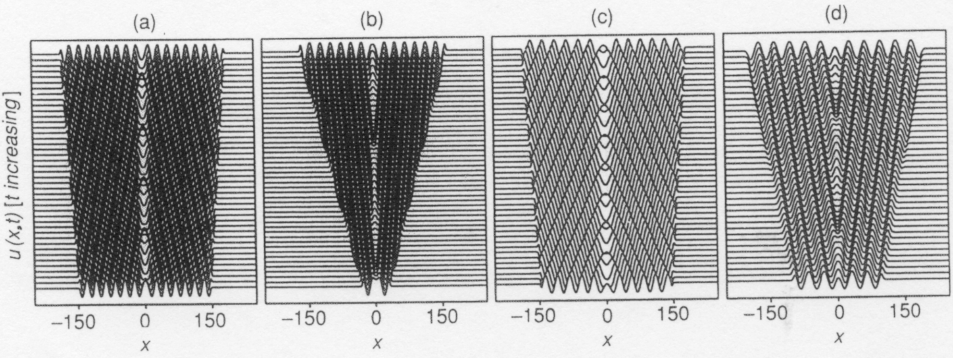

FIG. 3. The solution of (1.1) subject to (1.2) for a variety of functional forms of $\lambda(\cdot)$ and $\omega(\cdot)$. In each case I plot u as a function of x at successive times, with the vertical separation of solutions proportional to the time interval. The solution for v is qualitatively very similar. The solution consists of an amplitude transition wave moving outwards from the origin, with periodic plane waves behind the front. In each case $L = 5$ and $\varepsilon = 0.01$, and the functional forms are: (a) $\lambda(r) = 3 - r^2e^r$, $\omega(r) = 4 - r^3$; (b) $\lambda(r) = 6 - e^r \log(1 + 4r)$, $\omega(r) = 1 - r^2$; (c) $\lambda(r) = 4 - e^r$, $\omega(r) = 6 - \log(1 + r)$; (d) $\lambda(r) = 1 - (r + r^2 + r^3 + r^4)$, $\omega(r) = 0.1 - r^2e^{3r}$. These forms are chosen for their variety, and have no special significance. The time intervals over which the solutions are plotted are: (a) $40 \leq t \leq 50$; (b) $5 \leq t \leq 30$; (c) $40 \leq t \leq 50$; (d) $50 \leq t \leq 100$.

Transition fronts of constant shape and speed in r and θ_x have the form $(r, \theta_x) = (\hat{r}(x-ct), \hat{\psi}(x-ct))$, where c is the front speed. To be specific I consider the waves in $x>0$ which are moving in the positive x direction, so that $c>0$. From (2.1b), $\theta_t \to \omega(0)$ far ahead of the front, which gives $\theta = \hat{\Psi}(x-ct) + \omega(0)t$, where $\hat{\Psi}(\cdot)$ is an indefinite integral of $\hat{\psi}(\cdot)$. Substituting these solution forms into (2.1) gives a third-order system of ordinary differential equations:

$$\hat{r}'' + c\hat{r}' + \hat{r}\lambda(\hat{r}) - \hat{r}\hat{\psi}^2 = 0, \qquad \hat{\psi}' + c\hat{\psi} + 2\hat{r}'\hat{\psi}/\hat{r} + \omega(\hat{r}) - \omega(0) = 0, \quad (2.4a,b)$$

where primes denote differentiation with respect to $z = x - ct$. In this form the equations are singular at $r=0$, and thus before analysing the system I follow Howard & Kopell (1974, 1977) and rewrite it in terms of $\hat{r}$, $\hat{\psi}$, and $\hat{\phi} = \hat{r}'/\hat{r}$:

$$\hat{r}' = \hat{r}\hat{\phi}, \qquad \hat{\phi}' = \hat{\psi}^2 - c\hat{\phi} - \hat{\phi}^2 - \lambda(\hat{r}), \qquad \hat{\psi}' = \omega(0) - \omega(\hat{r}) - c\hat{\psi} - 2\hat{\phi}\hat{\psi}. \quad (2.5a\text{–}c)$$

A number of previous authors have presented analytical methods for investigating bounded trajectories in systems of travelling wave ordinary differential equations for reaction–diffusion systems (e.g. Gardner 1982, 1984; Dunbar, 1983, 1986; Terman, 1988), and these methods may be amendable to the rather different system (2.5). However, I do not adopt this approach, but rather I consider only local behaviour near steady states, in combination with numerical evidence for trajectory paths.

3. The transition wave equations

In this section I investigate the system (2.5), with the goal of determining the possible speeds for transition fronts of r and θ_x, and the steady-state values behind these fronts, which correspond to periodic plane waves. Steady states of (2.5) with $\hat{r} \neq 0$ have $\hat{\phi} = 0$ and $\hat{\psi} = [\omega(0) - \omega(\hat{r})]/c$, with

$$c^2\lambda(\hat{r}) = [\omega(\hat{r}) - \omega(0)]^2. \quad (3.1)$$

When $\lambda(\cdot)$ and $\omega(\cdot)$ are both strictly decreasing, (3.1) has a unique solution, and this solution compares extremely well with the amplitude behind the r–θ_x transition wave in numerical solutions of (1.1). Following my previous notation, I denote this steady state by $(r_s, 0, \psi_s)$. Explicit determination of the stability matrix at this steady state shows that the eigenvalues μ satisfy

$$\mu^3 + 2c\mu^2 + \{c^2 + 4\lambda(\hat{r}_s) + \hat{r}_s\lambda'(\hat{r}_s)\}\mu + \frac{\hat{r}_s}{c}\frac{d}{d\hat{r}}\{c^2\lambda(\hat{r}) - [\omega(\hat{r}) - \omega(0)]^2\}\Big|_{\hat{r}=\hat{r}_s} = 0.$$

Therefore the sum of the eigenvalues is negative, while their product is positive, so that there is one real positive eigenvalue, with the other two having negative real part. Therefore there are exactly two trajectories originating from the steady state. I denote these trajectories by $T^{\pm}$, according to the sign of $\hat{\phi}$ for large

negative z. Numerical integration of (2.5) as an initial value problem, starting close to $(r_s, 0, \psi_s)$ on the unstable eigenvector, suggests that $\hat{r}$, $\hat{\phi}$, and $\hat{\psi}$ all tend to infinity on T^+, but that T^- remains bounded. To consider further the behaviour of T^- for large positive z, I investigate steady states of (2.5) for which $\hat{r} = 0$.

If $\hat{r}$ and $\hat{\psi}$ are both zero, then a steady state must have $\hat{\phi}^2 + c\hat{\phi} + \lambda(0) = 0$, which has real roots for $\hat{\phi}$ if and only if $c \geqslant 2\lambda(0)^{\frac{1}{2}}$. Conversely, if $\hat{r} = 0$ but $\hat{\psi} \neq 0$, then $\hat{\phi} = -\frac{1}{2}c$ and $\hat{\psi}^2 = \lambda(0) - \frac{1}{4}c^2$ at a steady state, which has real roots for $\hat{\psi}$ if and only if $c \leqslant 2\lambda(0)^{\frac{1}{2}}$. I consider first the case $c > 2\lambda(0)^{\frac{1}{2}}$. Then the steady states are $(0, \hat{\phi}_1, 0)$ and $(0, \hat{\phi}_2, 0)$, say, where $\hat{\phi}_2 < \hat{\phi}_1 < 0$. Straightforward calculation shows that the first of these is stable, while the second has one real negative and two real positive eigenvalues. Numerical integration of the equations (2.5) for a range of functional forms for $\lambda(\cdot)$ and $\omega(\cdot)$ suggests that T^- terminates at the stable equilibrium $(0, \hat{\phi}_1, 0)$ (Fig. 4(b)).

When $c < 2\lambda(0)^{\frac{1}{2}}$, the steady states are $(0, -\frac{1}{2}c, \pm[\lambda(0) - \frac{1}{4}c^2]^{\frac{1}{2}})$. These steady states have one real negative and two pure imaginary eigenvalues. The pure imaginary eigenvalues correspond to eigenvectors in the $\hat{\phi}$–$\hat{\psi}$ plane, and thus the corresponding behaviour can be investigated by considering (2.5b) and (2.5c) with $\hat{r} = 0$. Substituting

$$U = -(\hat{\phi} + \tfrac{1}{2}c)/[\lambda(0) - \tfrac{1}{4}c^2]^{\frac{1}{2}}, \qquad V = \hat{\psi}/[\lambda(0) - \tfrac{1}{4}c^2]^{\frac{1}{2}}, \qquad \zeta = z[\lambda(0) - \tfrac{1}{4}c^2]^{\frac{1}{2}},$$

this second-order system becomes

$$\mathrm{d}U/\mathrm{d}\zeta = 1 + U^2 - V^2, \qquad \mathrm{d}V/\mathrm{d}\zeta = 2UV. \tag{3.2a,b}$$

Therefore $U^2 - 2UV(\mathrm{d}U/\mathrm{d}V) = V^2 - 1$. Dividing by U^4 gives a first-order equation for V/U^2 as a function of V, which can be integrated to give $U^2 + (V \pm K)^2 = K^2 - 1$, where $K > 1$ is a constant of integration. Therefore the trajectories of (3.2) are all circles, centre $(0, \pm K)$ and radius $(K^2 - 1)^{\frac{1}{2}}$, and the steady states $(U, V) = (0, \pm 1)$ are true centres. In the full system (2.5), the behaviour near the steady state is therefore a stable eigenvector with a nonzero $\hat{r}$ component, coupled with a true centre in the $\hat{\phi}$–$\hat{\psi}$ plane. Numerical integration suggests that in this case T^- terminates on one of the periodic orbits in the $\hat{r} = 0$ plane (Fig. 4(a)).

Therefore, for c on both sides of the bifurcation value $2\lambda(0)^{\frac{1}{2}}$, the trajectory T^- is a connection between $\hat{r} = \hat{r}_s$ and $\hat{r} = 0$, and corresponds to a well-defined solution of the partial differential equations consisting of travelling fronts in r and θ_x. However, it remains to consider the stability of these solutions. I have been unable to solve the linear stability problem analytically, but numerical solutions suggest that the waves of speed $c < 2\lambda(0)^{\frac{1}{2}}$ are unstable as reaction–diffusion solutions, while those of speed $c \geqslant 2\lambda(0)^{\frac{1}{2}}$ are stable. Figure 5 illustrates the evolution of (1.1) using the trajectory T^- as an initial condition; the value of c affects the initial condition T^-, but the partial differential equations (1.1) are of course independent of c. For $c \geqslant 2\lambda(0)^{\frac{1}{2}}$, the transition wave form in r and θ_x persists, moving across the domain with speed c. In fact, I have previously presented numerical evidence suggesting that with initial conditions such that $u, v \sim \mathrm{e}^{-\xi x}$ as $x \to \infty$, with $\xi \geqslant \lambda(0)^{\frac{1}{2}}$, the reaction–diffusion solution evolves to

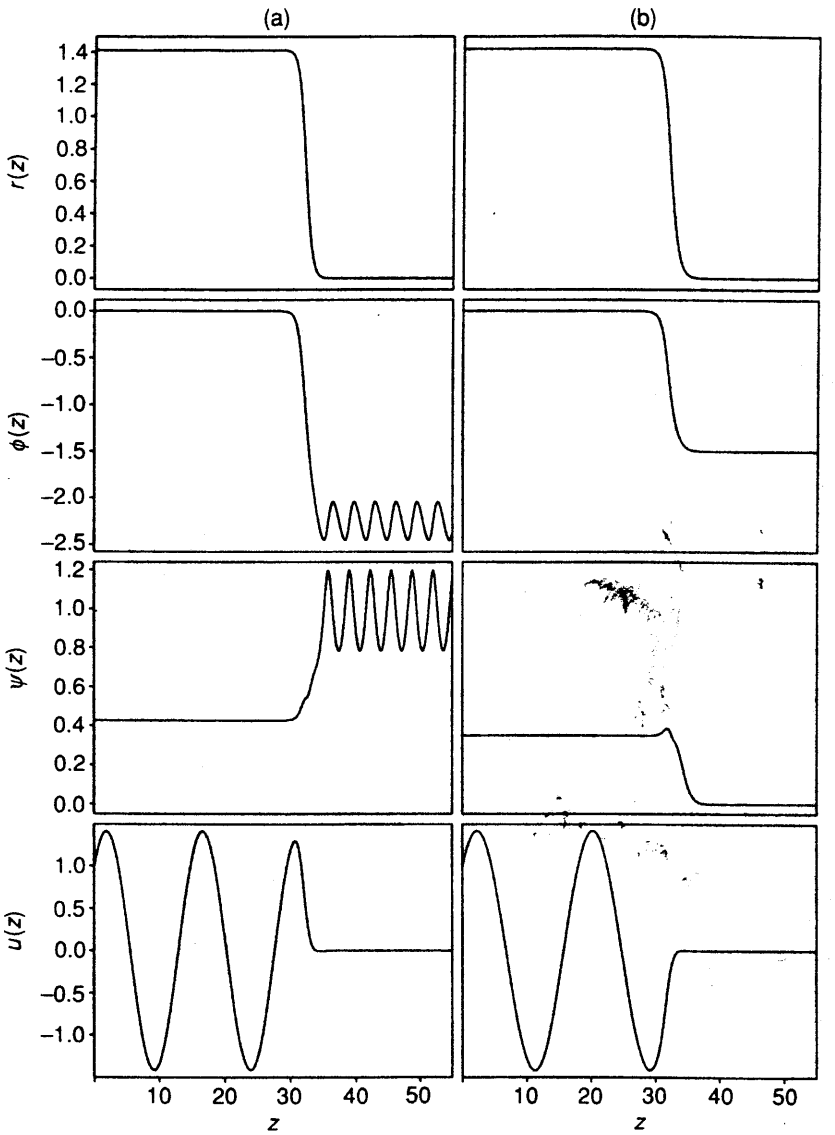

FIG. 4. Examples of the trajectory T^- in the system (2.5) for (a) $c < 2\lambda(0)^{\frac{1}{2}}$ and (b) $c > 2\lambda(0)^{\frac{1}{2}}$. I plot $\hat{r}, \hat{\phi}, \hat{\psi}$ as functions of z, and also the corresponding wave form for $u = \hat{r}(z)\cos[\hat{\Psi}(z)]$, where $\hat{\Psi}(\cdot)$ is an indefinite integral of $\hat{\psi}(\cdot)$. In the figure, $\lambda(r) = 6 - re^r$ and $\omega(r) = (1 + 3r^4)^{-1} + e^{-8r}$, so that the bifurcation wave speed $2\lambda(0)^{\frac{1}{2}} \approx 4.9$. In (a), $c = 4.5$, and in (b) $c = 5.5$. The trajectory was determined by integrating the system (2.5) numerically using a Runge–Kutta–Merson method, with initial values $(\hat{r}, \hat{\phi}, \hat{\psi}) = (\hat{r}_s, 0, \hat{\psi}_s) - \nu(e_1, e_2, e_3)$, where $0 < \nu \ll 1$ and (e_1, e_2, e_3) is the normalized unstable eigenvector of (2.5) at $(\hat{r}_s, 0, \hat{\psi}_s)$, with $e_2 > 0$.

transition waves in r and θ_x of speed $\xi + \lambda(0)/\xi$ (Sherratt, 1993a,b). This type of dependence on initial data is very similar to that in the Fisher equation (Rothe, 1978). However, if $c < 2\lambda(0)^{\frac{1}{2}}$, the initial condition T^- evolves to a front in r and θ_x moving with speed $2\lambda(0)^{\frac{1}{2}}$; the limiting shape of the front is simply the trajectory T^- when $c = 2\lambda(0)^{\frac{1}{2}}$.

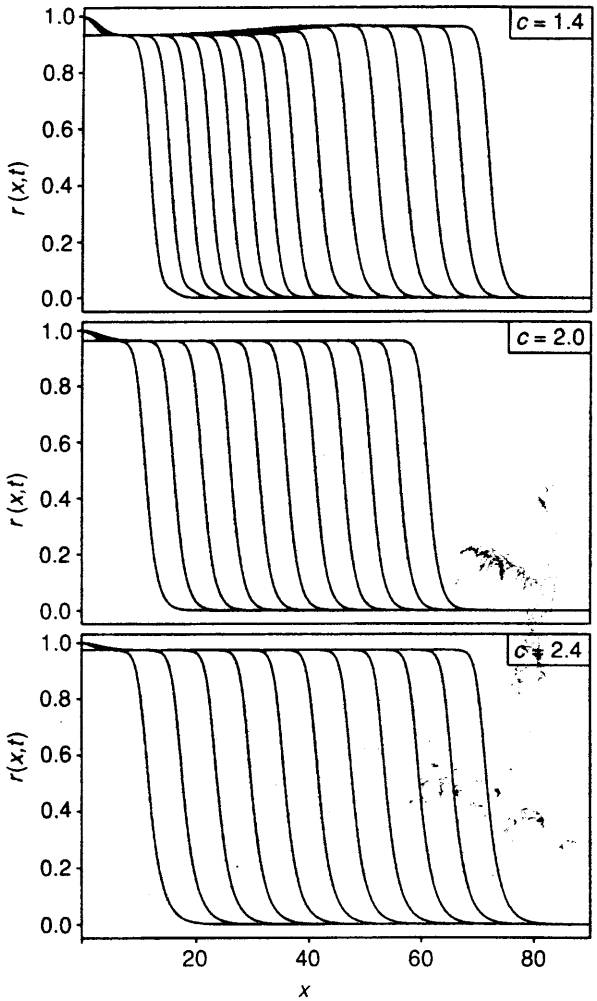

FIG. 5. The solution of (1.1) with the initial condition given by the trajectory T^- in the system (2.5), for three different values of c. I plot the solution amplitude r as a function of x at equally spaced times (time interval = 2.5). The trajectory T^- is an amplitude transition wave solution of (1.1), and was calculated as described in the legend to Fig. 4. This figure illustrates the general observation in numerical solutions that the transition wave T^- is stable as a partial differential equation solution for $c \geq 2\lambda(0)^{\frac{1}{2}}$, whereas for $c < 2\lambda(0)^{\frac{1}{2}}$ the wave is unstable, and the solution evolves to the wave with speed $2\lambda(0)^{\frac{1}{2}}$. In the figure, $\lambda(r) = 1 - r^6$ and $\omega(r) = 5 - r^3$, so that the bifurcation speed $2\lambda(0)^{\frac{1}{2}}$ is 2. The system (1.1) was solved numerically, subject to zero flux boundary conditions.

Returning now to evolution of (1.1) from (1.2) when L is small, numerical solutions for a range of functional forms for $\lambda(\cdot)$ and $\omega(\cdot)$ suggest that the transition waves in r and θ_x that develop in this case move with the minimum stable speed $2\lambda(0)^{\frac{1}{2}}$. This means that the amplitude r_s of the periodic plane waves behind this front is the unique solution of $4\lambda(0)\lambda(r_s) = [\omega(r_s) - \omega(0)]^2$. The velocity of the periodic plane waves is $-\omega(r_s)/\psi_s = 2\lambda(0)^{\frac{1}{2}}/[1 - \omega(0)/\omega(r_s)]$.

Since $\omega(\cdot)$ is strictly decreasing, this is always less than the front velocity $2\lambda(0)^{\frac{1}{2}}$; however, it can be negative with an absolute value greater than the front speed.

The evolution of transition waves moving with a minimum speed is reminiscent of behaviour in single reaction–diffusion equations. Kolmogoroff *et al.* (1937) studied the system $y_t = y_{xx} + F(y)$, where $F(y_1) = F(y_2) = 0$ with $F(y) > 0$ on (y_1, y_2), and $F'(y_1) > 0$ with $F'(y) < F'(y_1)$ on $(y_1, y_2]$. They showed that transition wave solutions with $y \geq y_1$ exist only for speeds greater than or equal to $2F'(y_1)^{\frac{1}{2}}$. In the vast majority of applications (reviewed by Murray, 1989: Chap. 9), the condition $y \geq y_1$ is necessary for the solution to be physically realistic: typically y is a population density and $y_1 = 0$. Moreover, Kolmogoroff *et al.* (1937) showed that for initial conditions such that $F(y(x, t = 0))$ has compact support in x, the partial differential equation solution evolves to the transition wave with the minimum possible speed $2F'(y_1)^{\frac{1}{2}}$. However, there is an important difference between this result for a single reaction–diffusion equation and the situation discussed here. For the system (1.1), $2\lambda(0)^{\frac{1}{2}}$ appears to be a minimum speed for *stability*, but waves of lower speeds do exist and *are* physically realistic, since the solution amplitude $r \geq 0$ for all z.

4. Larger scale perturbations

Having considered the cases of $L = \infty$ and L very small, I now investigate the solution of (1.1) subject to (1.2) when L is large but finite. From the discussions above, one would still expect transition waves in r and θ_x to move outwards, leaving periodic plane waves behind them. However, the difference in this case is that when a sufficiently large region of the domain is perturbed, the central part of that region is some distance from the amplitude transition wave, and evolves towards the limit cycle solution of the kinetics. A typical example of the subsequent behaviour is illustrated in Fig. 6. In addition to the transition wave in r and θ_x moving away from the initial disturbance with speed $c = 2\lambda(0)^{\frac{1}{2}}$, there is a second transition wave moving into the disturbance. Behind both fronts $r \to r_s$ and $\theta_x \to \psi_s$, corresponding to periodic plane waves in u and v. Ahead of the outward moving wave $r \to 0$, so that the system is at the steady state, while ahead of the inward moving wave $r \to r_L$ and $\theta_x \to 0$, so that the system is executing spatially homogeneous temporal oscillations.

I denote by s the velocity of the inward moving wave. Again I consider waves in $x > 0$, and I continue the sign convention that a positive velocity means a wave moving in the positive x direction, so that one expects $s < 0$. The inward moving wave then has the form $(r, \theta_x) = (\bar{r}(x - st), \bar{\psi}(x - st))$. Far ahead of the front (near the centre of the initial perturbation), $r \to r_L$ and $\theta_x \to 0$, so that (2.1b) implies that $\theta_t \to \omega(r_L)$. Therefore $\theta = \bar{\Psi}(x - st) + \omega(r_l)t$, where $\bar{\Psi}(\cdot)$ is an indefinite integral of $\bar{\psi}(\cdot)$. Substituting these solution forms into (2.1) gives a third-order system of ordinary differential equations:

$$\bar{r}'' + s\bar{r}' + \bar{r}\lambda(\bar{r}) - \bar{r}\bar{\psi}^2 = 0, \qquad \bar{\psi}' + s\bar{\psi} + 2\bar{r}'\bar{\psi}/\bar{r} + \omega(\bar{r}) - \omega(r_L) = 0. \quad \text{(4.1a,b)}$$

This system is different from the equations (2.4) for $\hat{r}$ and $\hat{\psi}$ because of the

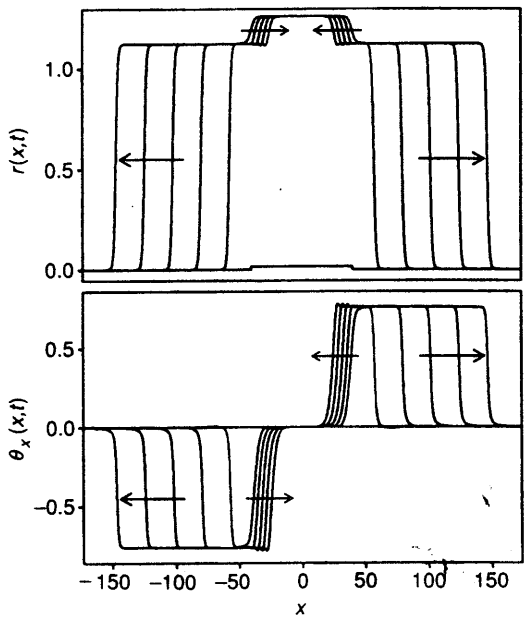

FIG. 6. The solution of (1.1) subject to (1.2) with $\lambda(r) = 2 - r^3$, $\omega(r) = 3.5/(1 + r^4)$, $L = 40$, and $\varepsilon = 0.01$. I plot r and θ_x as functions of x at equally spaced times, including $t = 0$; the time interval is 8. The system evolves to two sets of transition fronts in r and θ_x, one moving away from the perturbation, the other moving into it. The steady-state values between the fronts correspond to periodic plane waves in u and v.

different behaviour ahead of the front. Since $\lambda(r_L) = 0$, it follows that $(\bar{r}, \bar{\psi}) = (r_L, 0)$ is automatically a steady state of (4.1). However, the requirement that $(\bar{r}, \bar{\psi}) = (r_s, \psi_s)$ is a steady state determines the wave velocity s as

$$s = \frac{\omega(r_L) - \omega(r_s)}{\psi_s} = c\frac{\omega(r_l) - \omega(r_s)}{\omega(0) - \omega(r_s)}. \tag{4.2}$$

Under our assumption that $\omega(\cdot)$ is strictly decreasing, the value for s given by (4.2) has the opposite sign to c, so that the two fronts always move in opposite directions, as in Fig. 6. The value predicted by (4.2) agrees extremely well with that observed in numerical solutions of (1.1) for a wide range of functional forms for $\lambda(\cdot)$ and $\omega(\cdot)$.

As a slight digression, I now investigate the possibility that $s > 0$ when $\omega(\cdot)$ is not strictly decreasing. I do not make any attempt at a general study, but rather I consider the following specific functional forms for $\lambda(\cdot)$ and $\omega(\cdot)$:

$$\lambda(r) = 1 - r, \qquad \omega(r) = \omega_0 - 2[\beta r(\alpha - r)]^{\frac{1}{2}}, \tag{4.3}$$

where $\alpha > 1$ and $\beta > 0$ are real parameters. In this case $c = 2$, and the equation (3.1) has the unique solution

$$r_s = \frac{1}{2\beta}\{1 + \alpha\beta - [(1 + \alpha\beta)^2 - 4\beta]^{\frac{1}{2}}\}. \tag{4.4}$$

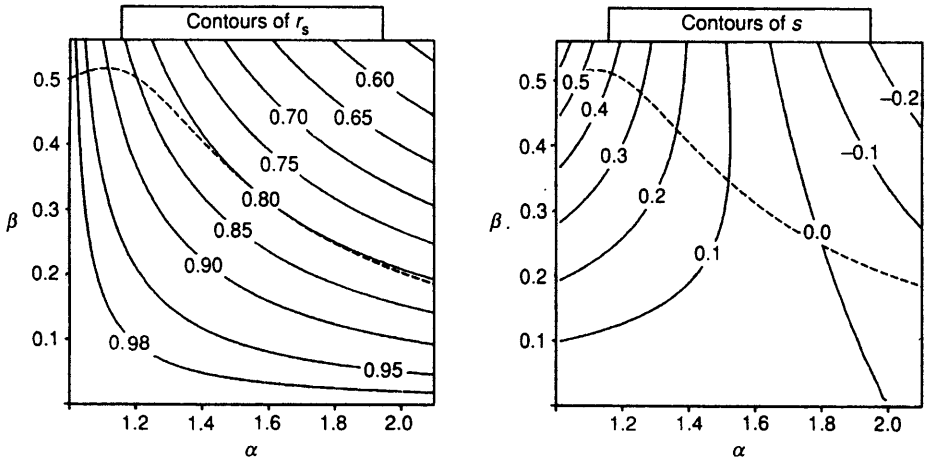

FIG. 7. Contour plots of r_s and s as functions of α and β when $\lambda(\cdot)$ and $\omega(\cdot)$ are given by (4.3). Expressions for r_s and s are given in (4.4) and (4.5) respectively. The periodic plane waves of amplitude r_s are stable if and only if β is below the dashed line, which is the curve $(16\beta - 5)(1 - r_s) = 4\alpha^2\beta^2 - 1$, calculated using (2.3).

Equation (4.2) implies that

$$s = 2\left[\left(\frac{\beta(\alpha - 1)}{1 - r_s}\right)^{\frac{1}{2}} - 1\right]. \tag{4.5}$$

The variation of r_s and s with α and β is illustrated in Fig. 7. In particular, (4.5) implies that s can be positive or negative, depending on α and β. When $s < 0$, numerical solutions of (1.1) subject to (1.2) with L large have the same qualitative form as the solution illustrated in Fig. 6. That is, two sets of transition fronts in r and θ_x move with constant shape and speed in opposite directions. Therefore, one expects intuitively that, when (4.5) gives $s > 0$, the solution will again evolve to two sets of transition fronts, both moving with constant shape and speed in the positive x direction. However, numerical solutions suggest that this is not the case (Fig. 8). Rather, there is a constant shape transition front connecting $(r, \theta_x) = (0, 0)$ and $(r, \theta_x) = (r_s, \psi_s)$, which does move with constant shape and speed as before, and there is also a second wave, which moves in the positive x direction, but not with constant shape. The form of the solution illustrated in Fig. 8 is qualitatively the same for a wide range of α, β, and ω_0 for which $s > 0$, and implies that the region in which the system executes spatially homogeneous temporal oscillations does not grow with time. Rather, this region remains of approximately constant width ($\approx 2L$), and the transition region between these homogeneous oscillations and the periodic plane waves gradually increases in width.

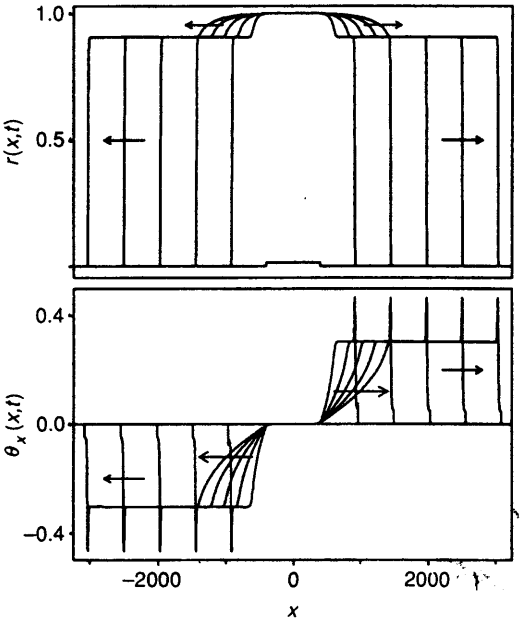

FIG. 8. The solution of (1.1) subject to (1.2) when $L = 400$, $\varepsilon = 0.01$, and $\lambda(\cdot)$ and $\omega(\cdot)$ are given by (4.3), with $\alpha = 1.1$, $\beta = 0.5$, and $\omega_0 = 1$. I plot r and θ_x as functions of x at equal spaced times, including $t = 0$; the time interval is 620. For these parameter values the wave speed s is positive, and the solution evolves two sets of waves in r and θ_x moving in the positive x direction. The leading wave moves with constant shape and speed (=2), but the trailing wave does not.

5. Conclusion

In contrast to scalar reaction–diffusion equations, the evolution of λ–ω systems from given initial data has received very little attention in the literature. In this paper, I have used a combination of analytical and numerical techniques to address this problem when the initial data has the particular form (1.2), and when $\lambda(\cdot)$ and $\omega(\cdot)$ are both strictly decreasing. I have shown that the solution evolves to two sets of transition wave fronts in the amplitude r and wave number θ_x, one moving outwards from the perturbation and one moving inwards. Numerical evidence suggests that the outwards moving wave has speed $2\lambda(0)^{\frac{1}{2}}$. I have shown analytically that at this wave speed there is a bifurcation in the form of amplitude transition waves for which $r \to 0$ ahead of the front, and I have presented numerical evidence suggesting that the stability of the waves changes at this bifurcation. I have also shown that the speed of the inward moving wave is uniquely determined by the speed of the outward moving wave. Between the transition fronts, the solution has the form of periodic plane waves for u and v, and their amplitude r_s is also determined by the speed of the outward moving transition front.

Linear stability of periodic plane waves as reaction–diffusion solutions can easily be determined using (2.3), and in Figs. 1–3, 6, and 8 I have deliberately chosen functional forms for which the periodic plane waves of amplitude r_s are

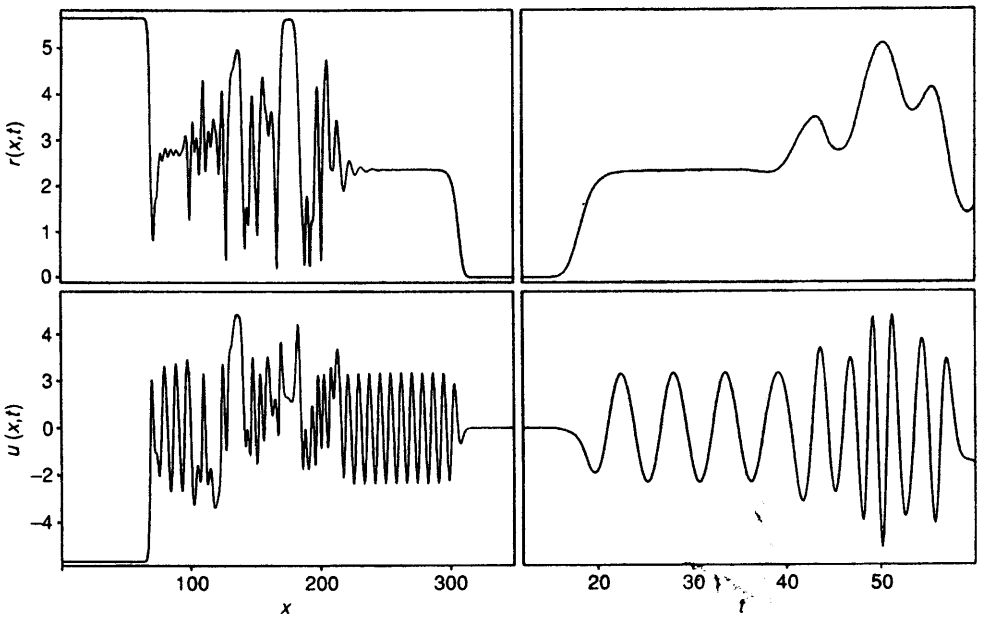

FIG. 9. The solution of (1.1) subject to (1.2) with $\lambda(r) = 2 - r^{0.4}$, $\omega(r) = 1 - r^{0.9}$, $L = 150$, and $\varepsilon = 0.01$. I plot r and u as functions of x at $t = 60$, and as functions of t at $x = 190$. In the former case, I plot only the region $x > 0$ for clarity; r and u are of course symmetric about $x = 0$. For these forms for $\lambda(\cdot)$ and $\omega(\cdot)$, (2.3) implies that the periodic plane waves with amplitude r_s are linearly unstable, and the waves between the amplitude transition fronts degenerate into irregular spatiotemporal oscillations.

stable. However, this is not always the case, and for some functional forms the front speed $c = 2\lambda(0)^{\frac{1}{2}}$ determines a plane wave amplitude for which the waves are unstable. I have solved the system (1.1) subject to (1.2) numerically for many such functional forms, and in each case the periodic plane waves degenerate into irregular spatiotemporal oscillations, as illustrated in Fig. 9. This is the case whether L is large or small. Typically there is a band of regular oscillations immediately behind the outward moving transition front, and there is in some cases a narrower band of regular oscillations immediately behind the inward moving front. The ability of λ-ω systems to sustain oscillations that are at least spatially irregular has been documented previously by Kopell & Howard (1981), who proved the existence of solutions that are temporally periodic but spatially irregular in systems for which $\lambda(\cdot)$ and $\omega(\cdot)$ are both strictly decreasing, with $\omega(\cdot)$ and $\omega'(\cdot)$ small. In the present case, the oscillations are not of this form because they are irregular in both space and time, and their precise nature is an open problem.

Acknowledgement

This research was supported in part by a Junior Research Fellowship from Merton College, Oxford.

References

DUNBAR, S. R. 1983 Travelling wave solutions of diffusive Lotka–Volterra equations. *J. Math. Biol.* **17**, 11–32.

DUNBAR, S. R. 1986 Travelling waves in diffusive predator–prey equations: Periodic orbits and point-to-periodic heteroclinic orbits. *SIAM J. Appl. Math.* **46**, 1057–78.

ERMENTROUT, G. B. 1980 Small amplitude stable wavetrains in reaction–diffusion systems. *Lect. Notes Pure Appl. Math.* **54**, 217–28.

GARDNER, R. A. 1982 Existence and stability of wave solutions of competition models: A degree theoretic approach. *J. Diff. Eqns.* **44**, 343–64.

GARDNER, R. A. 1984 Existence of travelling wave solutions of predator–prey systems via the connection index. *SIAM J. Appl. Math.* **44**, 56–79.

GREENBERG, J. M. 1981 Spiral waves for $\lambda-\omega$ systems. *Adv. Appl. Math.* **2**, 450–5.

HOWARD, L. N., & KOPELL, N. 1974 Wave trains, shock fronts, and transition layers in reaction–diffusion equations. *SIAM–AMS Proc.* **8**, 1–12.

HOWARD, L. N., & KOPELL, N. 1977 Slowly varying waves and shock structures in reaction–diffusion equations. *Stud. Appl. Math.* **56**, 95–145.

KOGA, S. 1982 Rotating spiral waves in reaction–diffusion systems. Phase singularities of multiarmed waves. *Prog. Theor. Phys.* **67**, 164–78.

KOLMOGOROFF, A., PETOVSKY, I., & PISCOUNOFF, N. 1937 Etude de l'équation de la diffusion avec croissance de la quantité de matière et son application à un problème biologique. *Moscow Univ. Bull. Math.* **1**, 1–25.

KOPELL, N., & HOWARD, L. N. 1973 Plane wave solutions to reaction–diffusion equations. *Stud. Appl. Math.* **52**, 291–328.

KOPELL, N., & HOWARD, L. N. 1981 Target patterns and horseshoes from a perturbed central force problem: Some temporally periodic solutions to reaction–diffusion equations. *Stud. Appl. Math.* **64**, 1–56.

LANGE, C. G., & LARSON, D. A. 1980 Transient solutions to some weakly diffusive nonlinear diffusion equations. *Stud. Appl. Math.* **63**, 249–62.

MURRAY, J. D. 1989 *Mathematical Biology.* Berlin: Springer.

ROTHE, F. 1978 Convergence to travelling fronts in semilinear parabolic equations. *Proc. R. Soc. Edin.* A **80**, 213–234.

SHERRATT, J. A. 1993a On the evolution of periodic plane waves in reaction–diffusion systems of $\lambda-\omega$ type. *SIAM J. Appl. Math.*, in press.

SHERRATT, J. A. 1993b The ampltude of periodic plane waves depends on initial conditions in a variety of $\lambda-\omega$ systems. *Nonlinearity*, in press.

TERMAN, D. 1988 Travelling wave solutions arising from a two-step combustion model. *SIAM J. Math. Anal.* **19**, 1057–80.